 doi:10.20944/preprints202011.0566.v2

Article

Self-Healing Biogeopolymers Using Biochar-Immobilized Spores of Pure- and Co-Cultures of Bacteria

Jadin Zam S. Doctolero [1], Arnel B. Beltran [1], Marigold O. Uba [3], April Anne S. Tigue [1] and Michael Angelo B. Promentilla [1,2,*]

[1] Chemical Engineering Department, Gokongwei College of Engineering, De La Salle University, Manila 1004, Philippines; jadin_doctolero@dlsu.edu.ph (J.Z.S.D.); arnel.beltran@dlsu.edu.ph (A.B.B.); april_tigue@dlsu.edu.ph (A.A.S.T.)

[2] Center for Engineering and Sustainable Development Research, De La Salle University, Manila 1004, Philippines; michael.promentilla@dlsu.edu.ph

[3] Biology Department, College of Science, De La Salle University, Manila 1004, Philippines; marigold.uba@dlsu.edu.ph

* Correspondence: michael.promentilla@dlsu.edu.ph; Tel.: +63-02-536-0223

Abstract: A sustainable solution for crack maintenance in geopolymers is necessary if they are to be the future of modern green construction. This study thus aimed to develop self-healing biogeopolymers that could potentially rival bioconcrete. First, a suitable healing agent was selected from *Bacillus subtilis*, *Bacillus sphaericus*, and *Bacillus megaterium* by directly adding their spores in the geopolymers and subsequently exposing them to a precipitation medium for 14 days. SEM-EDX analysis revealed the formation of mineral phases for *B. subtilis* and *B. sphaericus*. Next, the effect of biochar-immobilization and co-culturing (*B. sphaericus* and *B. thuringiensis*) on the healing efficiencies of the geopolymers were tested and optimized by measuring their ultrasonic pulse velocities weekly over a 28-day healing period. The results show that using co-cultured bacteria significantly improved the observed efficiencies, while biochar-immobilization had a weak effect but yielded an optimum response between 0.3-0.4 g/mL. The maximum crack width sealed was 0.65 mm. Through SEM-EDX and FTIR analyses, the biominerals precipitated in the cracks were identified to be mainly $CaCO_3$. With that, there is potential in developing self-healing biogeopolymers using biochar-immobilized spores of bacterial cultures.

Keywords: geopolymer; self-healing; crack repair; biomineralization; healing agent; ureolytic bacteria; non-ureolytic bacteria; co-cultured bacteria

1. Introduction

Geopolymers have become a promising greener alternative to concrete due to their low carbon footprint and excellent mechanical and chemical properties. They can be produced from a reaction involving an aluminosilicate source, which can come from waste byproducts like coal fly ash, and an alkaline solution that can induce the geopolymerization process. The use of different precursors and mix ratios has enabled several studies to report notable properties like high compressive/flexural strength, low shrinkage, acid and fire resistance, and high temperature and chemical stability in geopolymers [1-4]. However, being a cementitious material like concrete, they are still vulnerable to crack formation. This is undesirable, as it can cause the loss of structural integrity when geopolymers are used as materials of construction.

The traditional methods to repair cracks are often complex, expensive, and labor-intensive [5]. They can even be especially difficult to accomplish in hard-to-reach areas. Moreover, they must be

Preprints (www.preprints.org) | NOT PEER-REVIEWED | Posted: 30 November 2020 doi:10.20944/preprints202011.0566.v2

addressed as soon as they form to prevent further crack propagation. For this reason, self-healing has evolved as a promising solution to these problems. Past studies often favor the use of non-pathogenic soil microorganisms as healing agents because they are potentially safer and more sustainable than using chemical-based ones [6].

Bio-based self-healing occurs because when cracks form, air and water can reach the dormant microbes, activate them, and cause them to precipitate minerals which then seal the cracks [5, 6]. This process by which living forms influence the precipitation of minerals is known as biomineralization [7]. This phenomenon may be biologically induced or controlled depending on the species or agents used [8]. For biologically-induced mineralization, minerals are produced due to the metabolic activities of the microorganisms and the chemical reactions associated with the metabolic byproducts [9]. Its disadvantages are the poor crystallinity of the minerals, inclusion of impurities in their lattice structure, and the lack of control over mineral formation [10]. On the other hand, for biologically-controlled mineralization, the microorganisms exert more control in crystal formation due to the direct synthesis of the crystals at specific locations, yielding better crystalline structures [9]. However, it is through induced biomineralization in which more precipitates could be often produced in shorter periods of time [9].

By harnessing the capabilities of biologically-induced mineralization, huge progress has already been made for bio-based self-healing in cementitious materials, giving rise to bioconcrete [9, 11-14]. *Bacillus* bacteria are often employed because of their well-studied ability to form endospores and cause biomineralization. Despite these advancements, little is known whether the same methods used to make bioconcrete can also work for a geopolymer, which inherently has a different physico-chemical structure. It can also be more deleterious for microbial growth. At present, very few studies exist that explore the use of microorganisms in geopolymers for self-healing applications and enhancement of mechanical properties. Related studies are summarized in Table 1.

Table 1. Related studies on microbial applications on geopolymers.

Geopolymer Precursor	Healing Agent	Key Findings	Year of Publication	Reference
Metakaolin	*Sporosarcina pasteurii*	Sealing of 89±3-μm crack widths with $CaCO_3$	2018	[15]
Fly Ash	Solution of *S. pasteurii* and yeast from a fungi	Geopolymer pores were filled with $CaCO_3$, causing improvements in their mechanical properties	2018	[16]
Fly Ash	Genetically-modified *B. subtilis*	70.9%, 40.0%, and 68.87% increase in compressive strength, ultrasonic pulse velocity, and acid resistance, respectively, after 28 days	2019	[17]
Fly Ash	Solution of *S. pasteurii* and *Rhizopus oligosporus*	43.75% increase in compressive strength; higher amount of closed porosity for all specimens with microbes	2021	[18]

Given the huge gap that needs to be filled in truly developing self-healing biogeopolymers, the present study seeks to explore what locally available species of bacteria can be used as healing agents for fly ash-based geopolymers and how their viability in such a material can be further improved. The two factors that were tested to improve bacterial viability are immobilization and co-culturing.

Immobilization of bacteria spores before adding them to a concrete mixture has been reported to increase the survivability of bacteria in a cementitious matrix over a longer period of time [5]. This

Preprints (www.preprints.org) | NOT PEER-REVIEWED | Posted: 30 November 2020 doi:10.20944/preprints202011.0566.v2

is because of the additional layer that serves as a protection from external stresses, such as the mechanical strains during mixing. A study mentions that biochar has the potential to be used as an immobilizer because of its pore structure, which can house the bacteria spores, and its high affinity for fluid absorption and retention [13].

As for co-culturing, it was reported that a ureolytic bacteria and a non-ureolytic one can synergize to boost the biomineralization of $CaCO_3$ [19]. This is due to the surface of the non-ureolytic bacterial cells acting as additional nucleation sites for the Ca^{2+} ions to combine with CO_3^{2-}. In addition, it was also observed that the combined respiration rate of the two bacteria species reduced the alkalinity of the environment they were in. As a result, their viability in concrete greatly improved.

To the best of the authors' knowledge, immobilization and co-culturing bacteria has not been tested yet in developing self-healing geopolymers using microorganisms. With that, the present study finds relevance in building on a potential method to synthesize self-healing biogeopolymers.

2. Materials and Methods

2.1. Materials

The bacteria used for the screening of a suitable healing agent were *B. subtilis* BIOTECH 1679, *B. sphaericus* BIOTECH 1272, and *B. megaterium* BIOTECH 1512. The non-ureolytic species used for making the co-cultures was *B. thuringiensis* BIOTECH 1092. These bacteria were obtained from the Philippine National Collection of Microorganisms.

The geopolymer precursor employed was class F coal fly ash (FA) that was obtained from a coal-fired power plant in Bataan, Philippines. The alkaline activator (AA) was a constant mixture of Na_2SiO_3 and 12 M NaOH at a mass ratio of 2.5. The immobilizer utilized was rice-husk biochar which was obtained from the Philippine Rice Research Institute.

2.2. Equipment

The main equipment used were the Scanning Electron Microscope with Energy-Dispersive X-ray (SEM-EDX; Dual Beam Helios Nanolab 600i at FESEM accelerating voltage of 5.0 kV, FESEM beam current of 0.17 nA, EDS accelerating voltage of 15.0 kV, and EDS beam current of 0.69 nA; samples were gold-sputtered prior to testing), X-ray Diffractometer (XRD; Multiflex Rigaku Automated Powder XRD), X-ray Fluorescence Spectrophotometer (XRF; Shimadzu Model EDX-720), Fourier-Transform Infrared Spectrometer (FTIR; Perkin Elmer Frontier 100 via attenuated total reflection), and Ultrasonic Pulse Velocity Equipment (UPV; Proceq Pundit Lab+ UPV CT-133 using 150 kHz transducers).

2.3. Methods

2.3.1. Initial Characterization

The fly ash was first sieved using a 2-mm sieve screen to remove the large particles. After which, information regarding its elemental and mineral composition was obtained using energy-dispersive XRF and XRD. This is shown in Figure 1. Given the percent composition of silicon and aluminum in the table, the fly ash used could be considered a good aluminosilicate precursor for geopolymerization. Meanwhile, the XRD analysis indicates that quartz (SiO_2), mullite ($3Al_2O_3 \cdot 2SiO_2$), hematite (Fe_2O_3), and magnetite (Fe_3O_4) were present in the fly ash.

Preprints (www.preprints.org) | NOT PEER-REVIEWED | Posted: 30 November 2020 doi:10.20944/preprints202011.0566.v2

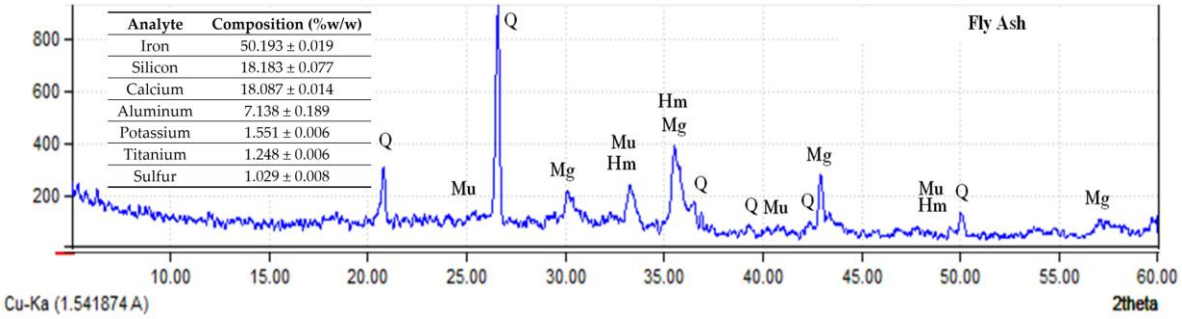

Figure 1. Elemental and mineral composition of the coal fly ash.

The biochar was also analyzed in terms of its morphology and elemental composition via SEM-EDX. This is presented in Figure 2. Its pore structure is evident which is beneficial for effectively housing and protecting the bacteria spores from external stresses. The pores were measured to be around 4.5-9.1 μm, which is bigger than the typical size of the *Bacillus* spores (around 1-2 μm). The biochar pores are also advantageous for holding water, a key requirement for promoting bacterial viability. As for its elemental composition, it is mainly rich in carbon, as the process of pyrolysis typically leaves behind a carbon-rich residue.

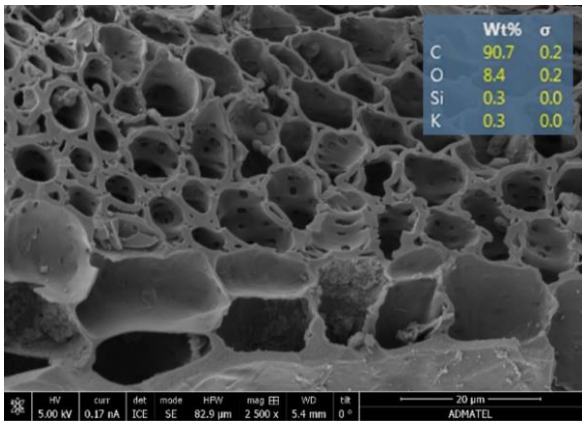

Figure 2. SEM-EDX analysis of biochar at 2500x magnification.

2.3.2. Preparation of Spore Suspensions

The spore suspensions of *B. subtilis*, *B. sphaericus*, and *B. megaterium* were made by first culturing them in separate sporulation mediums (13 g/L nutrient broth solutions with 10 mg/L of $MnSO_4 \cdot H_2O$) at 35ºC and 100 rpm agitation in a shaker bath for 7 days. After which, the broths were subjected to a heat shock treatment. This involved sudden immersion at 80ºC for 10 minutes followed by immediate cooling in an ice-water bath for 5 minutes. Next, the spores were harvested at 6,000 rpm for 15 minutes using a centrifuge. The spores were then washed twice with isotonic saline solution. From the spores collected, the spore suspensions (optical density of 2.0 at 600-nm setting) were made. These were subsequently pasteurized at 80ºC for 20 minutes before storing them at 4ºC. The Schaeffer-Fulton method was used to verify spore formation, and the stain results are shown in the appendix.

2.3.3. Selection of a Suitable Healing Agent

The geopolymer mixture was first made by mixing AA and FA at a mass ratio of 0.39. After thorough mixing, 6 mL of one of the three pre-prepared spore suspensions was added for every 95 g of AA used. These ratios were based on modifications of previous studies done on optimal geopolymer mix ratios for workability and compressive strength [20] and on making self-healing concrete [21]. The resulting mixture was then cast into the 50-mm cubic molds. Control specimens were also created. For these geopolymers, distilled water was added instead of a spore suspension.

Preprints (www.preprints.org) | NOT PEER-REVIEWED | Posted: 30 November 2020 doi:10.20944/preprints202011.0566.v2

Once the cubes had partially hardened, a 1-mm width slice was made at the top to simulate a single 1-mm crack. After 24 hours, the cubes were demolded and immersed in a precipitation medium (38.5 g/L urea broth and 5.6 g/L $CaCl_2$) for 14 days. From the results, only one suitable healing agent was selected for use in the two-factor test.

2.3.4. Two-Factor Test on Immobilization and Co-Culturing

The two factors tested in this phase were the type of culture (pure culture vs. co-culture) and the concentration of the biochar in the spore suspensions (low level of 0 g/mL and high level of 0.70 g/mL). Design-Expert® (V11) was used to generate the experimental design involving a categorical factor and a numerical factor. This is presented in the appendix. Essentially, the bacteria-containing geopolymers were composed of fly ash, activator, spore suspension with or without biochar, and nutrient solution. For the control specimens, the only difference was that distilled water was used instead of the spore suspensions.

To prepare the co-cultures, *B. thuringiensis* was grown together with the previously selected healing agent in the same sporulation medium [19]. The same methods discussed in Section 2.3.2 were then applied to make the spore suspensions. To immobilize the spores, biochar was added to the suspensions, and the mixtures were placed in an orbital shaker for 1 hour at 140 rpm to allow sufficient soaking [13]. As for the nutrient solutions, these were made by supplementing 20 g/L of urea and 5.6 g/L of $CaCl_2$ to nutrient broth.

Following the preparation of the suspensions and nutrient solutions, the geopolymers were made using the same mix ratios in Section 2.3.3. The nutrient solution was added last to the mixture. The mixtures were then cast into 50-mm cubic molds. There were three replicates for every treatment/control group. After 24 hours, the cubes were demolded and subjected to oven curing at 60ºC for 1 day to induce more natural cracks via thermal stress. This was then followed by six days of ambient curing (average temperature of 30ºC) by leaving the specimens exposed to open air.

Afterwards, the geopolymers were subjected to a dry-wet cycle (20 hours underwater and 4 hours air-drying) for 14 days and complete water immersion for the next 14 days. To non-destructively measure the changes in the geopolymers' mechanical properties, UPV measurements (using 150-kHz transducers) were taken every 7 days for the duration of the 28-day healing period.

2.3.5. Characterization of the Geopolymers and Biominerals

Finally, material characterization studies were performed. FTIR analysis was first done on the fly ash and a geopolymer specimen. Then, SEM-EDX and FTIR analyses were carried out to check for the presence of mineral phases in the collected precipitates from the geopolymer cracks and to determine their possible composition.

3. Results and Discussion

3.1. A Suitable Healing Agent for Geopolymers

The geopolymers with *B. subtilis*, *B. sphaericus*, and *B. megaterium* were observed after 14 days of immersion in the precipitation medium to select a suitable healing agent that could be used. It was observed that all those geopolymers exhibited no sealing of the induced cracks. However, upon closer inspection using an optical microscope, trace amounts of mineral-like structures were observed on the crack surfaces of the geopolymers with *B. subtilis* and *B. sphaericus*. At 10,000x magnification using an SEM, the presence of crystalline structures that were beginning to form were found. This could be attributed to the bacteria's cellular metabolism affecting the extracellular solution, leading to mineral precipitation [7-9]. The EDX analysis is shown in Figure 3. Due to the insufficient production of biominerals in the geopolymer cracks at this stage of the research, a proper analysis could not be performed to verify their true identities or composition. Nonetheless, there is initial evidence that biomineralization has occurred for the geopolymers with *B. subtilis* and *B. sphaericus*.

Preprints (www.preprints.org) | NOT PEER-REVIEWED | Posted: 30 November 2020 doi:10.20944/preprints202011.0566.v2

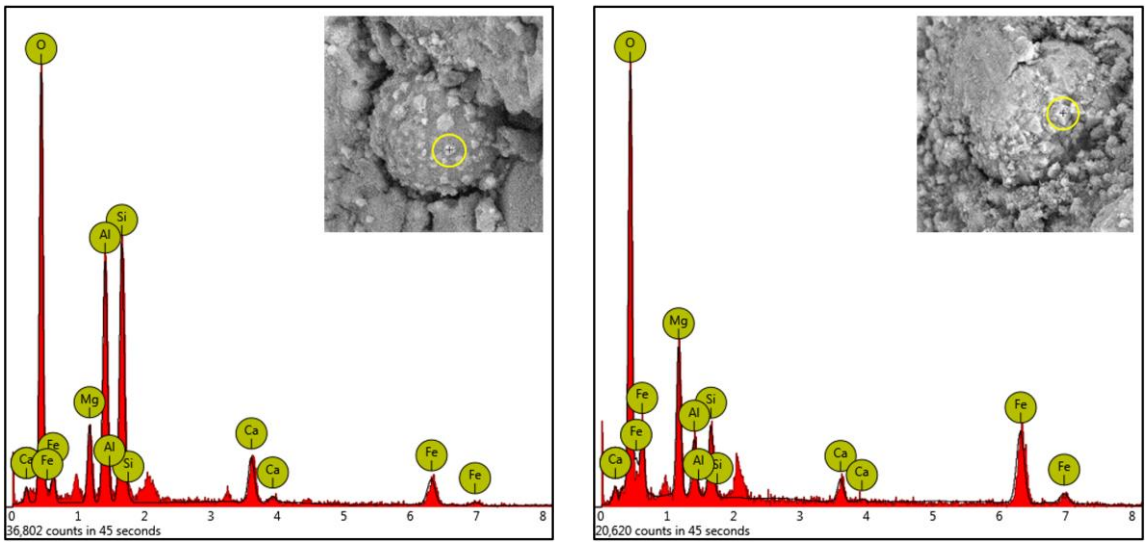

(**a**) (**b**)

Figure 3. EDX analysis of the minerals on the geopolymer with (**a**) *B. subtilis*; (**b**) *B. sphaericus*.

For this study, only one healing agent from *B. subtilis* or *B. sphaericus* could be further tested. For the succeeding two-factor test, *B. sphaericus* was the selected bacteria, as it has been mentioned in a previous study that it performs significantly better than *B. subtilis* in improving a material's mechanical properties [22].

3.2. Effect of Biochar-Immobilization and Co-Culturing

3.2.1. Test Results for the Control Geopolymers

The results for the control geopolymers are presented first to serve as a point of comparison for the findings for the bacteria-containing geopolymers. Through physical inspection of the control specimens, no precipitates were found that sealed the induced cracks. The changes in their mechanical properties were obtained next by comparing their UPV after cracking but before the healing period and after 28 healing days. UPVs work as a non-destructive measure of a material's quality by allowing ultrasonic waves to pass through it. The faster these waves travel, which happens when there are less cracks or voids in the material, the better the quality of the specimen.

The obtained mean healing efficiencies (percent improvement from the initial UPV after 28 healing days) are summarized in Table 2. It can be seen that the control specimens underwent an improvement of 2-3% despite the absence of bacteria. This could be attributed to the ongoing geopolymerization within the specimens even after curing for a total of 7 days. The same phenomenon could actually be also observed in concrete, wherein the hydration reactions continue to strengthen the material for roughly 28 days. Despite the limited curing time of the geopolymers which resulted to the observed healing efficiencies in Table 2, the data for the bacteria-containing specimens can still be justified by considering the largest improvement of 2.70% as the limit for which "healing" is only due to the ongoing geopolymerization.

Table 2. Healing efficiencies of the control geopolymers based on UPV measurements.

Control Group	Biochar Concentration (g/mL)	Mean Healing Efficiency (%)
Con-A	0	2.12
Con-B	0.175	2.33
Con-C	0.525	2.70
Con-D	0.7	2.61

Preprints (www.preprints.org) | NOT PEER-REVIEWED | Posted: 30 November 2020 doi:10.20944/preprints202011.0566.v2

3.2.2. Test Results for the Bacteria-Containing Geopolymers

Physical inspection of the bacteria-containing geopolymers after 28 healing days provided a completely different result than the one observed for the control groups. It was observed that all the bacteria-containing geopolymers exhibited crack closures, albeit to varying degrees. Figure 4 shows the biominerals precipitated in the cracks for the representative geopolymers with pure- and co-cultures of bacteria. The physical characteristics of the precipitates differed from the efflorescence products on the surface of the geopolymers; thus, they are likely to have materialized due to biologically-induced mineralization.

For the geopolymers with co-cultures, sealing of crack widths ranging from 0.10 mm to 0.65 mm were observed, while for those with pure cultures, it was only up to 0.35 mm. With this observation, the use of co-cultures can be said to be more effective on the basis of solely crack sealing.

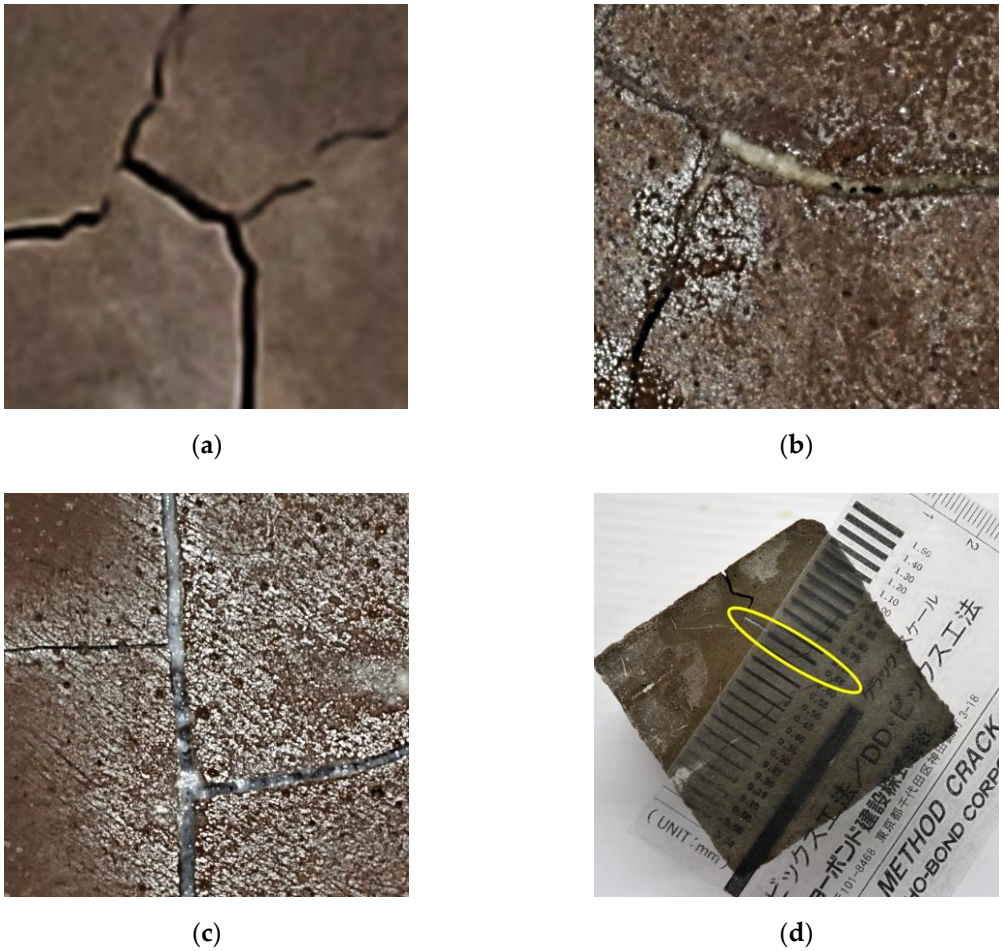

Figure 4. Crack sealing in a geopolymer after 28 healing days: (**a**) control specimen; (**b**) using pure culture; (**c**) using co-culture; (**d**) maximum crack width sealed.

When cracks in a cementitious material are sealed, its continuity naturally improves, giving rise to the observed strength developments over time. This is because the air gaps in it are gradually replaced with solid materials, leading to a greater compaction. The more compact the test specimen, the higher is the expected UPV value and quality of the material. UPV measurements were thus used to non-destructively describe the restoration of the lost mechanical properties. The healing efficiencies were obtained similarly with the control specimens as previously discussed. This can be found in Table 3.

A summary of the mean healing efficiencies in Table 3 is shown in Figure 5. The red points indicate the efficiencies for the geopolymers with pure cultures, while the green ones are for those with co-cultures. The dashed lines indicate the 95% confidence interval. The statistical analysis for this model and for the two-factor test results is presented in the appendix.

Preprints (www.preprints.org) | NOT PEER-REVIEWED | Posted: 30 November 2020 doi:10.20944/preprints202011.0566.v2

Table 3. Healing efficiencies of the bacteria-containing geopolymers based on UPV measurements.

Run	Biochar Concentration (g/mL)	Type of Culture	Mean Healing Efficiency (%)
1	0	Pure Culture	7.15
10	0.0945	Pure Culture	7.38
4	0.35	Pure Culture	7.55
7	0.35	Pure Culture	7.75
9	0.35	Pure Culture	7.91
6	0.6055	Pure Culture	7.91
3	0.7	Pure Culture	7.51
8	0	Co-Culture	9.97
13	0	Co-Culture	7.61
2	0.175	Co-Culture	13.23
5	0.35	Co-Culture	12.30
14	0.35	Co-Culture	10.30
11	0.525	Co-Culture	11.21
12	0.7	Co-Culture	9.79
15	0.7	Co-Culture	7.83

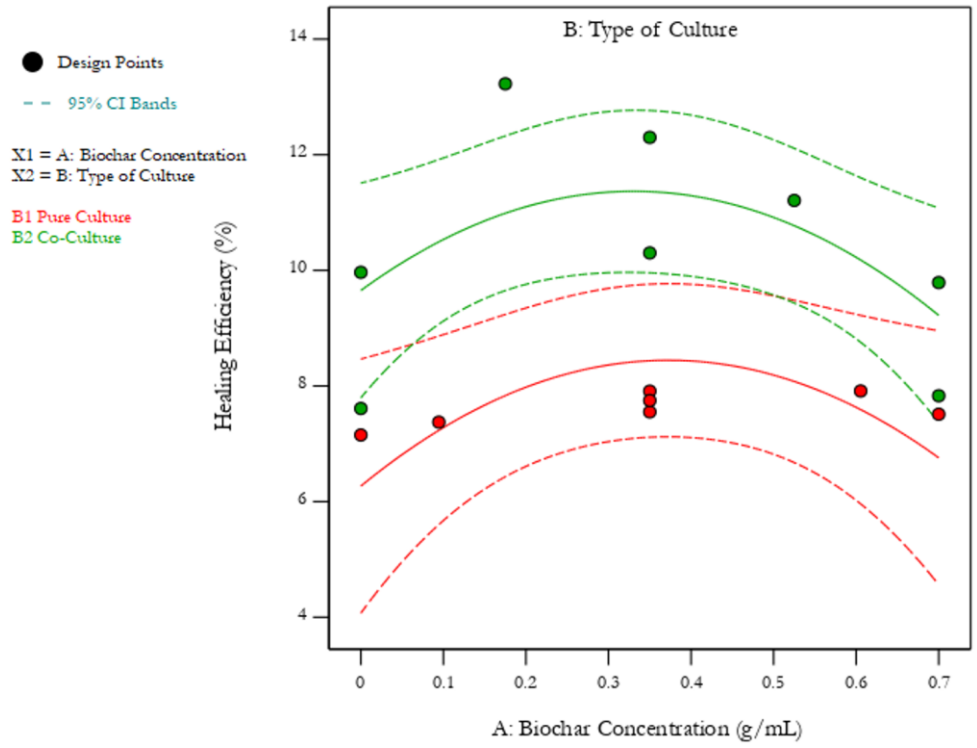

Figure 5. Graphical model on the effects of biochar-immobilization and co-culturing.

It can be seen from Figure 5 that changing the type of culture used caused the healing efficiencies to considerably increase. This can be easily visualized by looking at the green curve above the red one. Moreover, statistical analysis also points out that it has a p-value way lower than 0.05, making it highly significant. This supports the previous study done showing that co-culturing ureolytic and non-ureolytic bacteria has a synergistic effect on their biomineralization activity [19]. A theoretical explanation for this is that when the surfaces of the *B. sphaericus* cells were saturated with minerals, the cells of *B. thuringiensis* served as additional nucleation sites for further mineral production [19]. This could have led to the wider range of crack widths healed. However, further study is needed to examine the nucleation sites themselves.

Preprints (www.preprints.org) | NOT PEER-REVIEWED | Posted: 30 November 2020 doi:10.20944/preprints202011.0566.v2

Changing the biochar concentration, on the other hand, yielded a p-value above 0.05, making it insignificant. Thus, increasing the amount of biochar used to immobilize a given volume of spore suspension did not strongly contribute to the changes in the healing efficiencies of the geopolymers. However, looking at Figure 5, minor rises could still be observed in the healing efficiencies upon increasing the biochar loading. The response peaks at a certain point, then it decreases upon further loading. A possible explanation for this behavior is that the biochar initially serves as an additional protective layer for the spores, thereby increasing their viability in the geopolymers and causing the efficiencies to increase. It was also noted by a similar study that using a carrier material like biochar can aid in the distribution of spores within a specimen, ensuring the availability of bacteria spores at a crack site [13]. However, at higher biochar concentrations, their cellular metabolism could have been adversely affected by the increased interaction of the biochar with the microbes [23]. This could be further explored in future studies.

For both factors considered, the healing efficiencies obtained were well above the limit established from the results gathered from the control geopolymers. Therefore, the observed improvements in the properties of the bacteria-containing geopolymers arose because of biomineralization and not from the ongoing geopolymerization. Optimization of the two factors yielded a maximum healing efficiency of 11.37% using 0.33 g/mL of biochar and co-cultured bacteria. The solutions are illustrated in Figure 6.

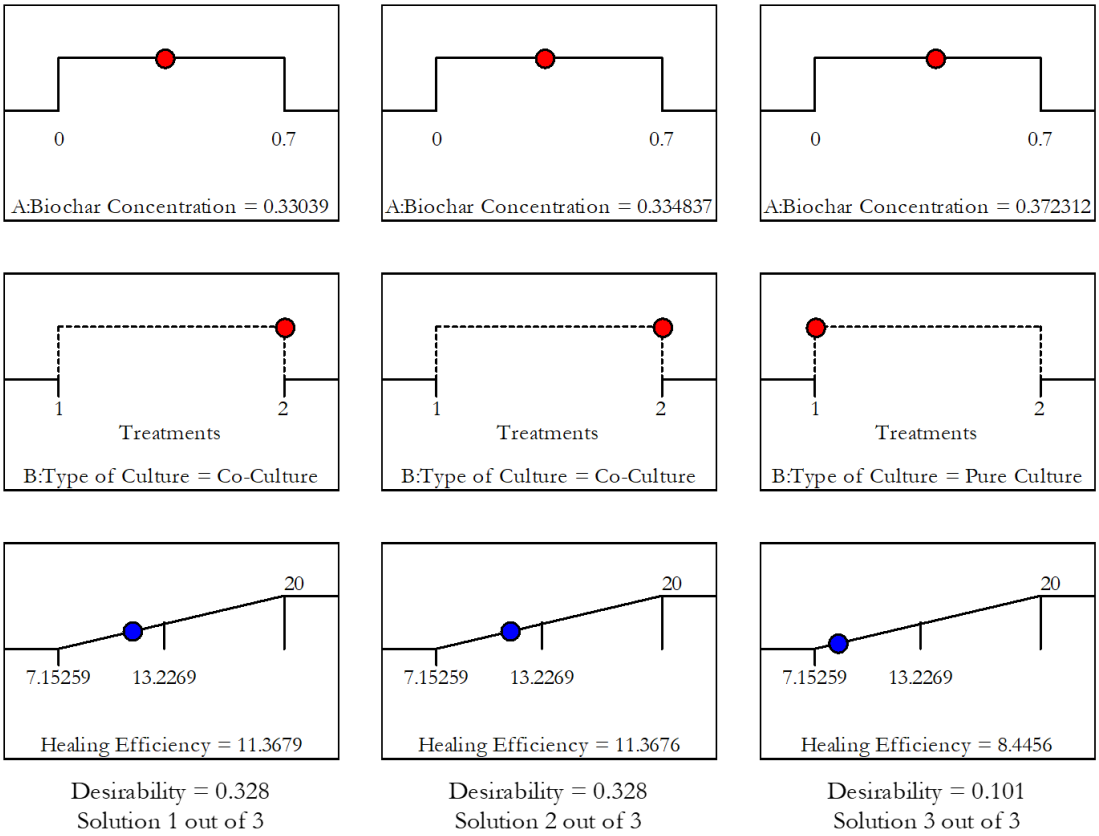

Figure 6. Solutions for the optimal healing efficiencies.

3.3. Characterization of the Geopolymers and Biominerals

3.3.1. Confirmation of Samples as Geopolymers

The bond properties of a geopolymer made in this study were studied through FTIR. Figure 7 shows the plots for the fly ash and a representative geopolymer in the study. A shifting can be observed from 1018 cm^{-1} in the fly ash to 994 cm^{-1} in the geopolymer. A shift towards a decreasing wavenumber in this region is an indication that geopolymerization occurred [3, 24].

Preprints (www.preprints.org) | NOT PEER-REVIEWED | Posted: 30 November 2020 doi:10.20944/preprints202011.0566.v2

It can also be seen that the geopolymer has a broad peak around 1000 cm^{-1}. This wavenumber is assigned to Si-O-Al and Si-O-Si vibrations and asymmetric stretching [25]. The band around this area is the most characteristic for geopolymers [26]; thus, this provides crucial evidence that the samples were indeed geopolymers. Second, peaks between 700-870 cm^{-1} indicate the presence of either tetrahedral or octahedral Al-O groups [27]. This is the result of variations in the structural reorganization of the reactive species as the geopolymerization process happens [27]. Third, peaks between 3300-3400 cm^{-1} and around 1650 cm^{-1} are due to the O-H asymmetric stretching due to the presence of water and silanol groups [25]. Lastly, the peak around 1400 cm^{-1} comes from the C-O groups in the CO_3^{2-} ions, which could have originated from the glass particles in the fly ash, from the added nutrient solution, or from the precipitated minerals.

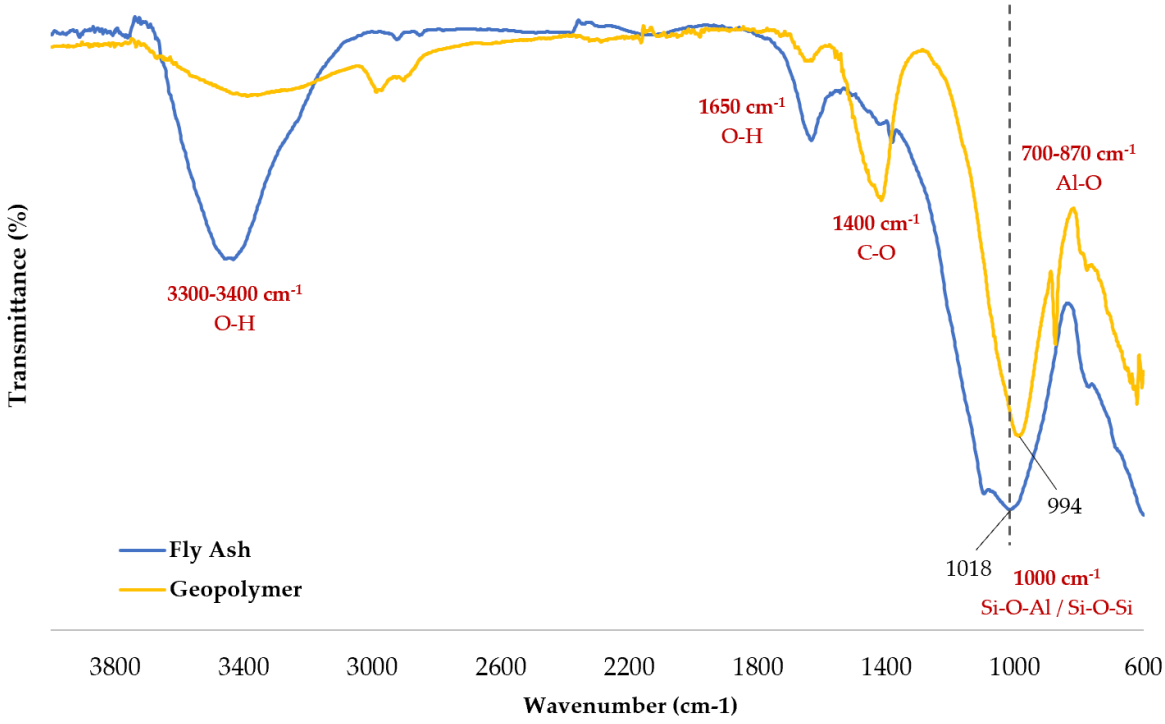

Figure 7. FTIR spectrum for the fly ash and for a control geopolymer.

3.3.2. Analysis of the Precipitates from Microbially-Induced Mineralization

The precipitates in the geopolymer cracks were removed and collected, and an SEM analysis was conducted. The images are shown in Figure 8. The presence of organized and well-defined structures in the sample can be seen. EDX analysis of the sample consistently gave an elemental composition of mainly calcium, oxygen, and carbon, as shown in Figure 9. This highly suggests that the precipitated mineral is most likely calcium carbonate ($CaCO_3$). However, since the self-healing process essentially involved a biologically-induced mineralization, the inclusion of impurities in their lattice structure and the lack of control over their mineral formation were expected [10]. This is evident from the subsequent FTIR analysis.

Preprints (www.preprints.org) | NOT PEER-REVIEWED | Posted: 30 November 2020 doi:10.20944/preprints202011.0566.v2

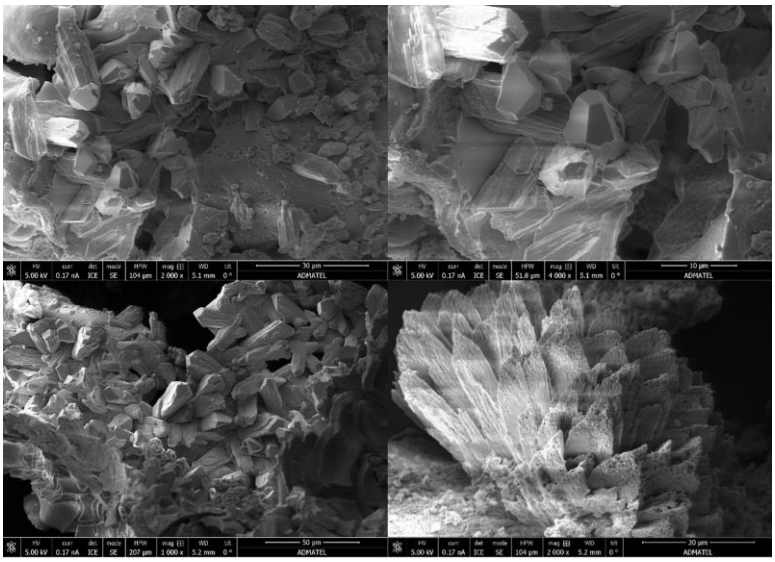

Figure 8. SEM images of the precipitates in the geopolymer cracks.

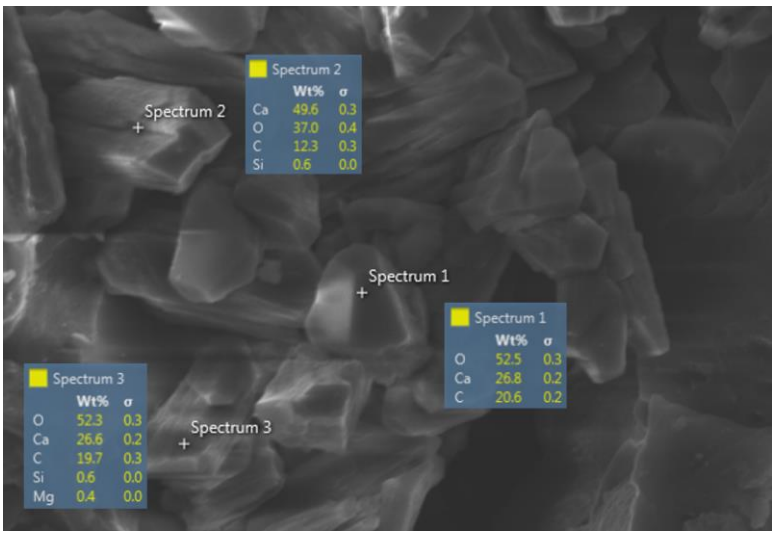

Figure 9. Elemental composition of the biominerals via EDX analysis.

The FTIR spectrum of the precipitates in the geopolymer cracks is shown in Figure 10. Through data matching, the composition was identified to be mainly calcite ($CaCO_3$). The key infrared vibrational bands (υ_{1-4}) of the carbonate ions are shown as well in the figure. It can also be seen in the plot that a broad water band is present. This is an indication that there might be amorphous materials mixed in with the sample. Those materials could be organic ones such as occluded bacterial cells. As previously stated, this is a common phenomenon for induced mineralization. Nonetheless, there is enough evidence to say that the geopolymer cracks were sealed with calcium carbonate.

Preprints (www.preprints.org) | NOT PEER-REVIEWED | Posted: 30 November 2020 doi:10.20944/preprints202011.0566.v2

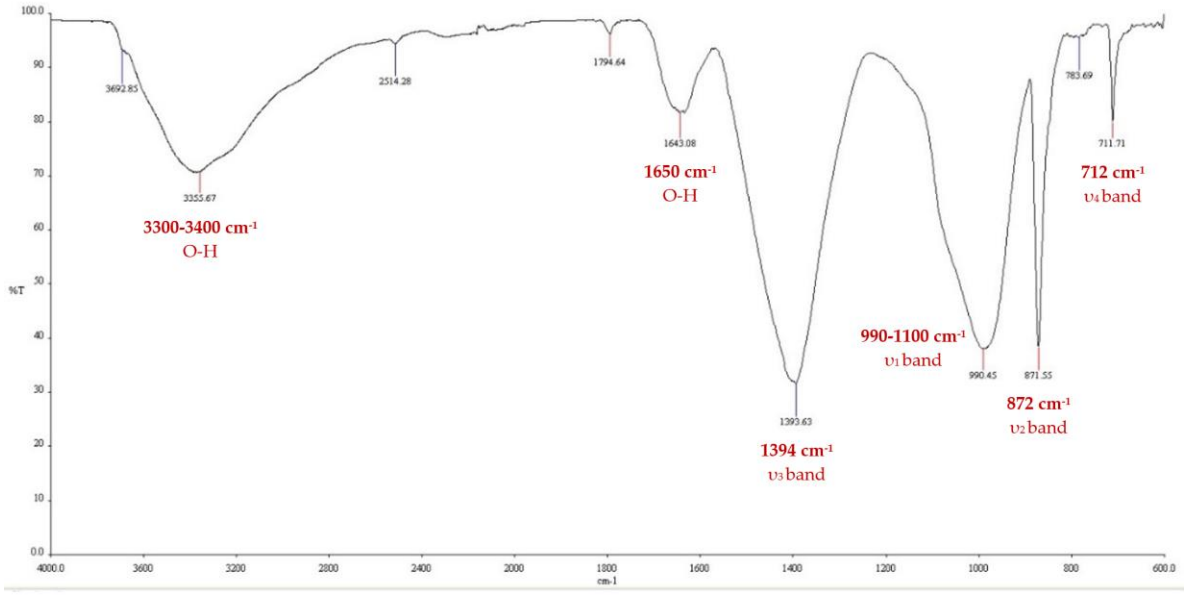

Figure 10. FTIR spectrum for the precipitates in the geopolymer cracks.

4. Conclusions

This study presents key findings in developing self-healing biogeopolymers. First, it was determined that both *B. subtilis* and *B. sphaericus* demonstrate the potential to act as healing agents for fly ash-based geopolymers. Despite the highly alkaline environment to which they were subjected, they remained viable and were found to cause the precipitation of mineral phases. In using *B. sphaericus* as the healing agent, it was found that co-culturing it with *B. thuringiensis* yields significantly higher healing efficiencies based on ultrasonic pulse velocity measurements of the geopolymers. This could be attributed to the synergistic action of a ureolytic and a non-ureolytic bacteria in the biomineralization of $CaCO_3$. The maximum crack width sealed was 0.65 mm as opposed to only 0.35 mm when pure cultures were used. Changing the biochar concentration to immobilize the spores, on the other hand, was found to have a weak effect. Despite that, a maximum response was attained when biochar concentration between 0.3-0.4 g/mL was used. Through material characterization studies, the biominerals were confirmed to be mostly calcite. With the observed physical sealing of the cracks and the recorded improvements in the mechanical properties of the geopolymers, self-healing could be said to have indeed occurred. Future work will consider the use of X-ray computed microtomography to visualize and directly measure the extent of self-healing in three dimensions [28, 29].

Moving forward, it is recommended to widen the scope of the optimization studies to determine the most optimal conditions for microbial viability and to obtain even higher healing efficiencies that were already attained in past research [17, 18]. Other researchers can look at the use of other microorganisms, immobilizing materials, geopolymer precursors, and mix ratios. It is also important to determine whether the weakening effect caused by the added bacteria and nutrients could be compensated by the strengthening effect brought about by self-healing. To gain more insights on the effect of the microorganisms on the strength parameters of the geopolymers, destructive tests are recommended to be used in tandem with non-destructive ones. With these future studies, biogeopolymers may eventually surpass bioconcrete and be gradually used in more practical applications where it can be seen as the concrete solution to a concrete problem on building more sustainable cities and communities.

Author Contributions: Conceptualization, formal analysis, and funding acquisition, J.Z.S.D. and M.A.B.P.; methodology, J.Z.S.D., A.B.B., M.O.U., and M.A.B.P.; writing—original draft preparation, J.Z.S.D.; writing—review and editing, J.Z.S.D., A.B.B., M.O.U., A.A.S.T., and M.A.B.P.; supervision, A.B.B., M.O.U., A.A.S.T., and M.A.B.P. All authors have read and agreed to the published version of the manuscript.

Funding: This research was funded by the Philippines' Department of Science and Technology – Engineering Research and Development for Technology (DOST-ERDT) and the Philippine Council for Industry, Energy, and Emerging Technology Research and Development (DOST-PCIEERD).

Acknowledgments: The authors acknowledge the Philippine National Collection of Microorganisms (PNCM), the Philippine Rice Research Institute (PhilRice), GNPower Mariveles Coal Plant Ltd. Co, Advanced Device and Materials Testing Laboratory (ADMATEL), Industrial Technology Development Institute (DOST-ITDI), and the DLSU iNano Research Facility for the materials and services provided for this research.

Conflicts of Interest: The authors declare no conflict of interest.

 doi:10.20944/preprints202011.0566.v2

Appendix A: Experimental Design for the Two-Factor Test

Table A1 shows the experimental design for the bacteria-containing geopolymers in the two-factor test of the study. This was generated using Design Expert by setting the following parameters: (a) pure culture as low level and co-culture as high level for type of culture, and (b) 0 g/mL as low level and 0.70 g/mL as high level for biochar concentration. The nutrient solution to spore suspension volume ratio was kept constant at 1.5.

Table A1. Experimental design for the two-factor test.

Run	Grams of Biochar per mL of Spore Suspension	Type of Culture
1	0	Pure Culture
2	0.175	Co-Culture
3	0.7	Pure Culture
4	0.35	Pure Culture
5	0.35	Co-Culture
6	0.6055	Pure Culture
7	0.35	Pure Culture
8	0	Co-Culture
9	0.35	Pure Culture
10	0.0945	Pure Culture
11	0.525	Co-Culture
12	0.7	Co-Culture
13	0	Co-Culture
14	0.35	Co-Culture
15	0.7	Co-Culture

Table A2 shows the specifications for the control specimens. These did not contain the spore suspensions but only distilled water. The nutrient solution to distilled water volume ratio was kept constant at 1.5.

Table A2. Control groups for the two-factor test.

Control Group	Grams of Biochar per mL of Distilled Water
Con-A	0
Con-B	0.175
Con-C	0.525
Con-D	0.70

Appendix B: Schaeffer-Fulton Stains

A comparison of the Schaeffer-Fulton stains directly from an agar plate and from the spore suspensions is shown in Figure B1. It can be seen that the spores in the prepared suspensions were not associated with red vegetative cells. This indicates that the spores obtained had sufficiently matured and that the method of preparing them was satisfactory. The appearance of the green stain in the spores was due to the malachite green being forced into the endospores by heat. Upon the use of the decolorizer, the green stain was washed out from the cell walls but not from the spore walls. The use of safranin then allowed the vegetative cells to be viewed as red.

Preprints (www.preprints.org) | NOT PEER-REVIEWED | Posted: 30 November 2020 doi:10.20944/preprints202011.0566.v2

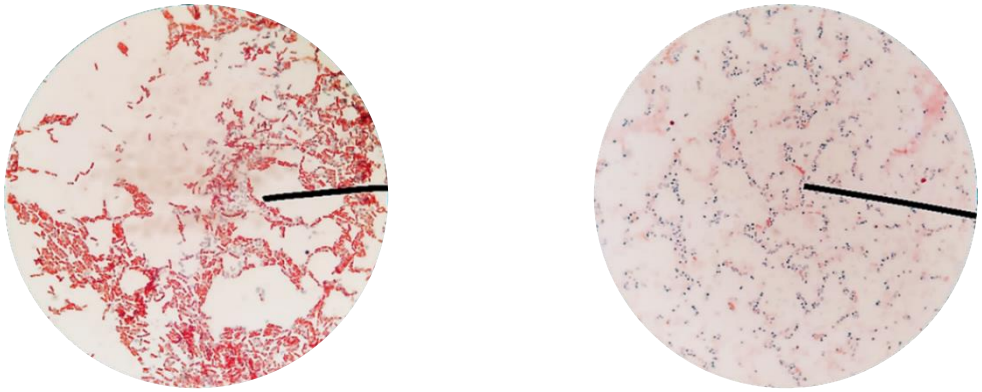

(**a**) (**b**)

Figure B1. Schaeffer-Fulton stains under an optical microscope: (**a**) directly from an agar plate; (**b**) from the spore suspensions.

Appendix C: Analysis of Variance for the Two-Factor Test

Figure C1 shows the ANOVA for the results of two-factor test. It shows that changes in the biochar concentration did not strongly affect the healing efficiencies of the geopolymers, but the use of co-cultures do. The analysis also shows that the model generated by the software is significant.

Source	Sum of Squares	df	Mean Square	F-value	p-value	
Model	37.73	4	9.43	5.63	0.0122	significant
A-Biochar Concentration	0.0017	1	0.0017	0.0010	0.9751	
B-Type of Culture	31.28	1	31.28	18.68	0.0015	
AB	0.3863	1	0.3863	0.2307	0.6413	
A^2	10.44	1	10.44	6.23	0.0316	
Residual	16.74	10	1.67			
Lack of Fit	9.99	5	2.00	1.48	0.3391	not significant
Pure Error	6.75	5	1.35			
Cor Total	54.47	14				

Figure C1. Analysis of variance for the two-factor test.

Figure C2 illustrates that the residual points lie close to the normal distribution line; thus, they follow a normal distribution. Furthermore, no other definite patterns can be observed from their plot. With that, no transformation of data was necessary.

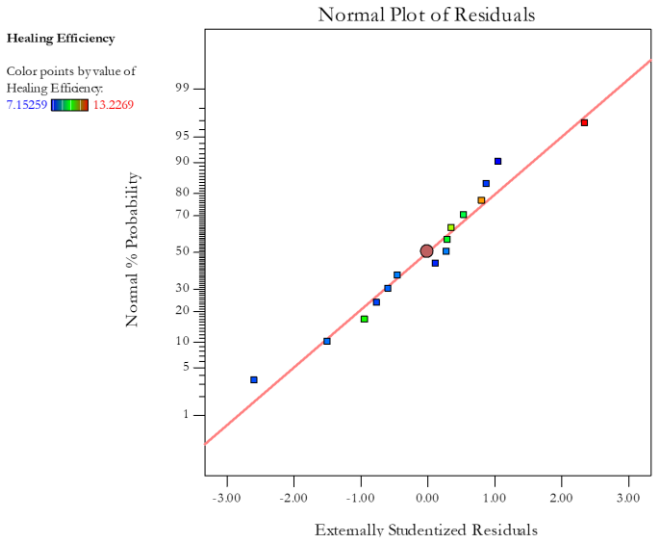

Figure C2. Normal plot of the residuals.

Preprints (www.preprints.org) | NOT PEER-REVIEWED | Posted: 30 November 2020 doi:10.20944/preprints202011.0566.v2

Figure C3 depicts the residuals versus the ascending predicted response values. Because the plot shows a random scatter and not an expanding variance, often identified by a "megaphone (<)" pattern, the assumption of constant variance was satisfied.

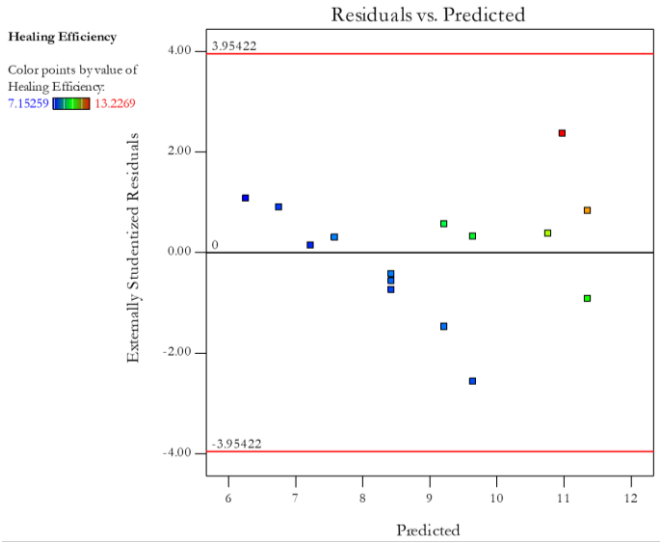

Figure C3. Plot of the residuals versus the predicted response values.

Figure C4 shows that the plots of the residuals versus biochar concentration and residuals versus type of culture show random scatter. This indicates that there is no systematic contribution of an independent factor not accounted for by the model.

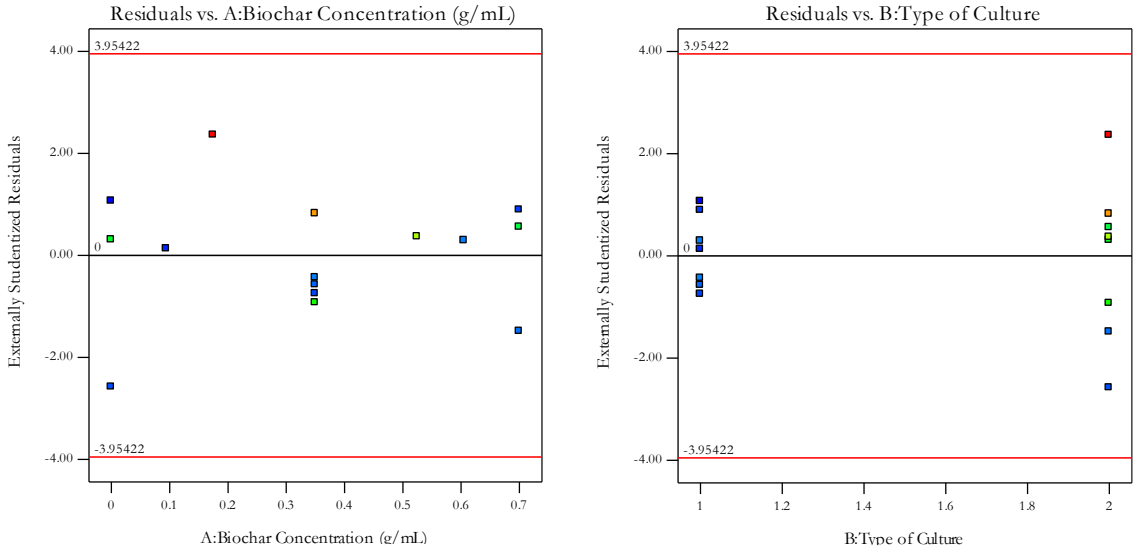

Figure C4. Plots of the residuals versus (**a**) biochar concentration and (**b**) type of culture.

References

1. Burciaga-Diaz, O., Magallanes-Rivera, R.X., & Escalante-Garcia, J.I. (2013). Alkali-activated slag-metakaolin pastes: Strength, structural, and microstructural characterization. *Journal of Sustainable Cement-Based Materials*, *2*(2), 111-127. https://doi.org/10.1080/21650373.2013.801799
2. Chi, M., Chang, J., & Huang, R. (2012). Strength and drying shrinkage of alkali-activated slag paste and mortar. *Advances in Civil Engineering*, *2012*. http://dx.doi.org/10.1155/ 2012/579732
3. Tigue, A., Malenab, R., Dungca, J., Yu, D., & Promentilla, M. (2018). Chemical stability and leaching behavior of one-part geopolymer from soil and coal fly ash mixtures. *Minerals*, *8*(9), 411. https://doi.org/10.3390/min8090411
4. Malenab, R., Ngo, J., & Promentilla, M. (2017). Chemical treatment of waste abaca for natural fiber-reinforced geopolymer composite. *Materials*, *10*(6), 579. https://doi.org/10.3390/ma10060579
5. Khaliq, W., & Ehsan, M.B. (2016). Crack healing in concrete using various bio influenced self-healing techniques. *Construction and Building Materials*, *102*, 349–357. https://doi.org/10.1016/j.conbuildmat.2015.11.006
6. Luo, J., Chen, X., Crump, J., Zhou, H., Davies, D. G., Zhou, G., … Jin, C. (2018). Interactions of fungi with concrete: Significant importance for bio-based self-healing concrete. *Construction and Building Materials*, *164*, 275–285. https://doi.org/10.1016/j.conbuildmat.2017.12.233
7. Skinner, H. C. W., & Ehrlich, H. (2014). Biomineralization. In Treatise on Geochemistry (pp. 105–162). Elsevier. https://doi.org/10.1016/b978-0-08-095975-7.00804-4
8. Benzerara, K. (2011). Biomineralization. In Encyclopedia of Astrobiology (pp. 197–198). Springer Berlin Heidelberg. https://doi.org/10.1007/978-3-642-11274-4_185
9. Dhami, N. K., Reddy, M. S., & Mukherjee, M. S. (2013). Biomineralization of calcium carbonates and their engineered applications: A review. *Frontiers in Microbiology*, *4*(OCT), 1–13. https://doi.org/10.3389/fmicb.2013.00314
10. Frankel, R., & Bazylinksi, D. (2013). Biologically induced mineralization by bacteria. *Reviews in Mineralogy and Geochemistry*, *54*(1), 95-114. https://doi.org/10.2113/0540095
11. Wang, J.Y., Snoeck, D., Van Vlierberghe, S., Verstraete, W., & De Belie, N. (2014). Application of hydrogel encapsulated carbonate precipitating bacteria for approaching a realistic self-healing in concrete. *Construction and Building Materials*, *68*, 110–119. https://doi.org/10.1016/j.conbuildmat.2014.06.018
12. Vijay, K., Murmu, M., & Deo, S.V. (2017). Bacteria based self-healing concrete – A review. *Construction and Building Materials*, *152*, 1008–1014. https://doi.org/10.1016/j.conbuildmat.2017.07.040
13. Gupta, S., Kua, H.W., & Pang, S.D. (2018). Healing cement mortar by immobilization of bacteria in biochar: An integrated approach of self-healing and carbon sequestration. *Cement and Concrete Composites*, *86*, 238–254. https://doi.org/10.1016/j.cemconcomp.2017.11.015
14. Mullem, T.V., Gruyaert, E., Caspeele, R., De Belie, N. (2020). First large scale application with self-healing concrete in Belgium: Analysis of the laboratory control tests. *Materials*, *13*(4), 997. https://doi.org/10.3390/ma13040997
15. Jadhav, U.U., Lahoti, M., Chen, Z., Qiu, J., Cao, B., & Yang, E.H. (2018). Viability of bacterial spores and crack healing in bacteria-containing geopolymer. *Construction and Building Materials*, *169*, 716–723. https://doi.org/10.1016/j.conbuildmat.2018.03.039
16. Wulandari, K.D., Ekaputri, J.J., Fujiyama, C., & Davin, H. (2018). Effects of microbial agents to the properties of fly ash-based paste. In *4th International Conference on Rehabilitation and Maintenance in Civil Engineering* (Vol. 195, pp. 12–15). MATEC Web of Conferences. https://doi.org/10.1051/matecconf/201819501012
17. Chatterjee, A., Chattopadhyay, B., & Mandal, S. (2019). Bacterium amended 100% fly ash geopolymer. In *International Conference on Sustainable Materials and Structures for Civil Infrastructures* (Vol. 2158, pp. 1–6). AIP Publishing. https://doi.org/10.1063/1.5127137
18. Wulandari, K. D., Ekaputri, J. J., Triwulan, Kurniawan, S. B., Primaningtyas, W. E., Abdullah, S. R. S., Ismail, N. 'Izzati, & Imron, M. F. (2021). Effect of microbes addition on the properties and surface morphology of fly ash-based geopolymer paste. *Journal of Building Engineering*, *33*, 101596. https://doi.org/10.1016/j.jobe.2020.101596
19. Son, H.M., Kim, H.Y., Park, S.M., & Lee, H.K. (2018). Ureolytic/Non-ureolytic bacteria co-cultured self-healing agent for cementitious materials crack repair. *Materials*, *11*(5). https://doi.org/10.3390/ma11050782

20. Arafa, S. A., Ali, A. Z., Awal, A. S., & Loon, L. Y. (2018). Optimum mix for fly ash geopolymer binder based on workability and compressive strength. In *Earth and Environmental Science*. IOP Publishing. https://doi.org/10.1088/1755-1315/140/1/012157
21. Nain, N., Deepa, T., Krishnamurthy, V., Tharannum, S., Surabhi, R., & Yathish, N. V. (2019). Enhancement in strength parameters of concrete by application of Bacillus bacteria. *Construction and Building Materials*, *202*, 904–908. https://doi.org/10.1016/j.conbuildmat.2019.01.059
22. Puranik, S.A., Jain, S., Sritam, G., & Sandbhor, S. (2019). Bacterial concrete – a sustainable solution for concrete maintenance. *International Journal of Innovative Technology and Exploring Engineering*, (11), 227–232. https://doi.org/10.35940/ijitee.K1046.09811S19
23. Gorovtsov, A. V., Minkina, T. M., Mandzhieva, S. S., Perelomov, L. V., Soja, G., Zamulina, I. V., Rajput, V. D., Sushkova, S. N., Mohan, D., & Yao, J. (2019). The mechanisms of biochar interactions with microorganisms in soil. *Environmental Geochemistry and Health*, *42*(8), 2495–2518. https://doi.org/10.1007/s10653-019-00412-5
24. Kalaw, M., Culaba, A., Hinode, H., Kurniawan, W., Gallardo, S., & Promentilla, M. (2016). Optimizing and characterizing geopolymers from ternary blend of Philippine coal fly ash, coal bottom ash and rice hull ash. *Materials*, *9*(7), 580. https://doi.org/10.3390/ma9070580
25. Khan, M., Azizli, K., Sufian, S., Siyal, A., Man, Z., & Ullah, H. (2014). Sodium silicate free geopolymer as coating material: adhesion to stell. In *International Electronic Conference on Materials*. https://doi.org/10.3390/ecm-1-b016
26. Rosas-Casarez, C., Arredondo-Rea, S., Gómez-Soberón, J., Alamaral-Sánchez, J., Corral-Higuera, R., Chinchillas-Chinchillas, M., & Acuña-Agüero, O. (2014). Experimental study of XRD, FTIR and TGA techniques in geopolymeric materials. *International Journal of Advances in Computer Science & Its Applications, 4*(4), 25-30. https://www.researchgate.net/publication/274079395
27. Kumay, S., & Kumar, R. (2010). Mechanical activation of fly ash: Effect on reaction, structure, and properties of resulting geopolymer. *Ceramics International*, *37*(2011), 533-541. https://doi.org/10.1016/j.ceramint.2010.09.038
28. Ruan, S., Qiu, J., Weng, Y., Yang, Y., Yang, E.-H., Chu, J., & Unluer, C. (2019). The use of microbial induced carbonate precipitation in healing cracks within reactive magnesia cement-based blends. *Cement and Concrete Research*, *115*, 176–188. https://doi.org/10.1016/j.cemconres.2018.10.018
29. Suleiman, A. R., Nelson, A. J., & Nehdi, M. L. (2019). Visualization and quantification of crack self-healing in cement-based materials incorporating different minerals. *Cement and Concrete Composites*, *103*, 49–58. https://doi.org/10.1016/j.cemconcomp.2019.04.026